ROSE 2013 - IEEE International Symposium on Robotic and Sensors Environments
Washington, DC, 21-23 October 2013

Instrumentation System for Ship Air Wake Measurement

Anil Kumar, Pinhas Ben-Tzvi, Murray R. Snyder, Wael Saab
Dept. of Mechanical and Aerospace Engineering
The George Washington University
Washington, DC USA
{anilinfotek, bentzvi, snydermr, waelsaab}@gwu.edu

***Abstract*— This paper presents an instrumentation system developed for off-ship measurement of ship air wakes using an instrumented radio controlled (RC) helicopter. We propose the use of an IMU as a sensor to measure air wake in the form of induced vibrations on the helicopter while it maneuvers through regions of active air wake. The proposed system makes use of Back Propagation neural networks to compensate for the vibrational noise contributed by pilot inputs. The instrumentation system was tested on a modified training vessel in the Chesapeake Bay, which provided a wide range of wind conditions.**

Keywords—Ship Air Wake, Artificial Neural Networks, RC Helicopter, Computational Fluid Dynamics

I. INTRODUCTION

Launch and recovery of rotary wing aircraft from naval vessels can be very challenging and potentially hazardous. Ship motion combined with the turbulence that is created as the wind flows over the ship's superstructure can result in rapidly changing flow conditions for rotary wing aircraft. Additionally, dynamic interface effects between the vessel air wake and the rotor wake are also problematic.

To ensure aircraft and vessel safety, launch and recovery envelopes are prescribed for specific aircraft types on different ship classes [1]. Permissible launch and recovery envelopes are often restrictive because of limited flight envelope expansion. Such flight envelopes are generally determined through flight testing which is frequently difficult to schedule, expensive, potentially hazardous and above all, highly subjective. Currently, the launch and recovery wind limits and air operation envelopes are primarily determined via the subjective analysis of test pilots. The simplest solution to such issues is complementary use of computational tools [2-8] to predict test conditions and extrapolate test results, thereby reducing the number of actual flight test points required. However, current computational methods are insufficiently validated for ships with a complex superstructure, such as a destroyer or cruiser. Validated computational air wake predictions can also be used for ship design and operational safety analysis. Therefore there is a need for non-subjective systems for experimental validations of CFD models for air wake patterns.

This research is funded by Office of Naval Research. Program Officer is Mr. John Kinzer (Code 351).

Most CFD validation methods available in the literature [9-13] are based on anemometer sensors, which are not suitable for off-ship air wake analysis. The most obvious reason is that, in tethered condition, it is not possible to measure air velocities from far distances, and in untethered condition (on some aircraft), high noise level limits accuracy in measurements.

II. PROPOSED SYSTEM

The proposed system makes use of a small remotely piloted helicopter (Fig. 1(b)) with rotor diameter of 1.3 m (4.5 ft) to measure air wake turbulence aft of the Naval Academy's YP676 flight deck (Fig 1(a)). The helicopter was equipped with a GPS and an IMU (Fig. 1(c)) for recording the position and vibrations of the helicopter as a function of time. The YP676 vessel was equipped with a reference anemometer and GPS for recording relative wind and the position of the boat. The helicopter was maneuvered through regions in the ship's air wake where steep velocity gradients exist. The lightweight (RC) helicopter was affected by the air wake turbulence where the velocity gradients appeared as noticeable vibrational patterns in the IMU's data [14]. Concurrently, the relative position of the helicopter was determined by comparing the GPS derived position of the helicopter with that of a reference position on the ship. Combining these two measurement systems, the locations of sharp gradients in the air wake can be mapped relative to the ship (accurate within one rotor diameter of the helicopter). Since the center of mass and the geometric center of the helicopter do not coincide, any wind gust during flight tends to rotationally oscillate the helicopter, which can be measured with a Gyroscope. As such, angular velocity measurements would provide better information about air wake compared to acceleration measurements. Therefore, an IMU with a gyroscope is an excellent sensor for measuring air wake intensity.

During underway flight operations, the YP's craft master attempted to keep the ship under the same relative wind over deck based upon the reference anemometer. This technique has one drawback where the IMU not only reads vibrations due to air wake, but also vibrations caused by the helicopter's own maneuvers which depends on pilot inputs. Therefore, to solely measure the air wake induced vibrational intensity, it is important to remove the contribution of pilot induced dynamic inputs from the IMU readings. Since the angular velocity is a vector quantity, the measurement from

Fig. 1: Experimental Setup: (a) YP676 training vessel (Top),(b) Instrumeted RC Helicoper on Deck (Middle), (c) IMU and GPS sensor (Bottom)

the IMU is basically a vector sum of the external disturbances and internal dynamics. If the IMU readings caused by pilot inputs alone can be estimated, the external disturbances (air wake) can be measured by subtracting the estimated readings from the actual readings. The proposed method uses a Back Propagation Neural Networks (BPNN) to predict the component of IMU readings arising from pilot inputs alone.

A Neural Network was trained to predict the IMU vibrational components due to pilot input. This predicted IMU data was subtracted from the actual measured data to obtain the actual disturbance due to air wake. For collection of training data, the helicopter was flown in a large enclosed room (USNA Rotor Lab), which was free of external disturbance (air wake and naturally imposed wind.) IMU data and pilot inputs were recorded during these flights. Fig 2 shows overall architecture of the proposed system for air wake measurement.

III. Pilot Input Compensation

The RC helicopter used for the experiments requires five dimensional pilot inputs. Three of which control swash plate dynamics and the remaining two control the tail rotor and throttle. Therefore, there are five Pulse Width Modulation (PWM) signals generated by the radio-

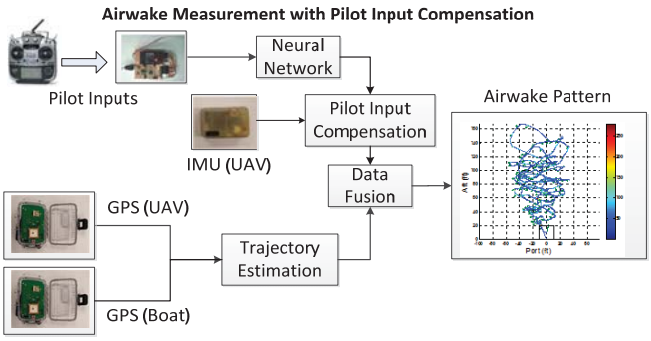

Fig: 2: System Architecture

controller as pilot inputs. Since the control signals from the radio transmitter (Remote Controller) are sent as 'one-to-all' broadcasting mode, multiple RF receivers can communicate with a single transmitter. Therefore, an additional RC receiver was used to read the control signals sent by the transmitter. A USB powered custom PCB (Fig. 3) was designed and integrated in order to read the required five PWM control channels at a refresh rate of 30 Hz.

IV. Modeling IMU Response to Pilot Inputs using Neural Networks

Artificial neural network (ANN) [15-18] is usually defined as a network composed of a large number of processing units (neurons) that are massively inter connected, operate in parallel and learn from experience (training samples). ANNs are widely used as a pattern recognition tool especially for nonlinear regression problems.

Fig. 3: Pilot Input Receiver Module

Back-Propagation Neural Network (BPNN) is a multilayer feed-forward network based on error back propagation algorithm [17-19].

A. Application of BPNN in Predicting Air wake

The proposed system approximates the pilot input data points (within a fixed time window) to a line and then uses the line parameters to describe the pilot input history. For each pilot input channel (total five), a history window of 15 samples (equivalent to 0.5 s of data) was modeled with a line

equation $y = mx + c$. Here y is the concerned pilot input channel sample, m is the slope, x is the sample index (equivalent to time) and c is the offset in this linear model. If N is the number of samples in the history window (N=15 in our case) then the parameters m and c are calculated using the least square method as follows:

$$m = \frac{N\sum_{i=1}^{N} x_i y_i - \sum_{i=1}^{N} x_i \cdot \sum_{i=1}^{N} y_i}{N\sum_{i=1}^{N} {x_i}^2 - \left(\sum_{i=1}^{N} x_i\right)^2}, \quad (1)$$

$$c = \frac{\sum_{i=1}^{N} {x_i}^2 \cdot \sum_{i=1}^{N} y_i - \sum_{i=1}^{N} x_i \cdot \sum_{i=1}^{N} x_i y_i}{N\sum_{i=1}^{N} {x_i}^2 - (\sum_{i=1}^{N} x_i)^2} \quad (2)$$

Since the pilot data is not a perfect fit to the linear model it is required to consider curve-fitting error while linearizing the pilot data. The proposed system uses sum of the absolute errors (e) as the third parameter for modeling pilot input data, which is calculated as follows:

$$e = \sum_{i=1}^{N} |y_i - (mx_i + c)|. \quad (3)$$

Three parameters {m, c, e} were obtained from each pilot input data channel. Five data channels resulted in 15 parameters to represent pilot input data signals.

In the proposed method, four channels of gyroscope data were used by BPNN. First three channels were Cartesian components of low pass filtered gyroscope data. The fourth predicted channel was the local standard deviation of the magnitude (in spherical coordinate system) of the Gyroscope data in a fixed sized window. Therefore, the Neural Network took a 15-dimensional input vector (i.e. pilot data) to predict a 4-dimensional output vector (i.e. gyroscope data).

The input and output layer had fixed number of nodes, i.e. 15 and 4 respectively because these are determined by the dimensionality of the input and the output data. The network topology for the hidden layers was selected using 'trial and error' method. It was found that the topology with 12 and 8 nodes respectively in the two hidden layers give the best prediction accuracy. Fig. 4 shows the final neural network topology used in the proposed method. A 10-fold cross validation [20] was implemented to prevent overtraining of the network.

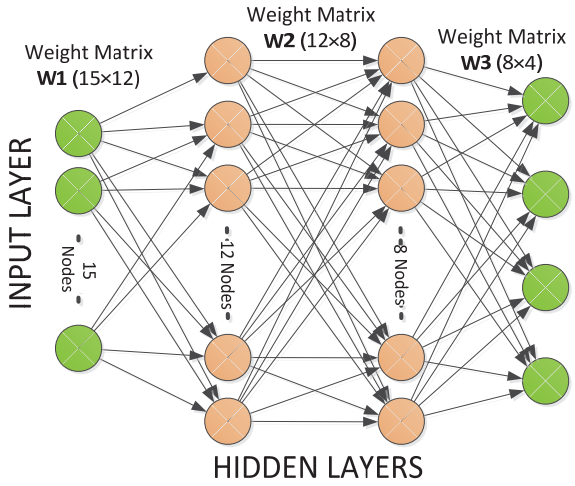

Fig. 4: Neural Network Topology used for predicting IMU output

B. *Network Performance*

Training the network consisted of collecting flight data from experiments conducted in a Rotor testing Lab in the US Naval Academy. The Rotor Lab provided an air wake /natural wind free zone for data collection. Data was collected from five flight conducted on three different helicopters (two Pro and one ESP TREX 600 models). Out of the three total flights conducted with the ESP model, two were used for training the neural network, which provided approximately a total of 37,000 data samples. One fourth of the total data was used for actually training the network. The accuracy of the network was assessed by testing it on a complete data set. The histogram chart in Fig. 5 plots the error in predicting IMU gyroscope data which indicates that the most probable error is ±2˚/sec. which is believed to be a good result given the noise produced by a flying helicopter. Fig. 6 shows prediction results of the neural network along with actual measurements. Ideally, there should be a perfect overlap between the actual measurement (in blue) and the predicted data (in red). In this case the predicted X and Y components of the gyroscope do not overlap very well with the actual measurements. This is because of the limited ability to vary the X and Y components of the gyroscope data as compared to the Z component due to limited space in the Rotor Lab and the need to ensure helicopter safety. Therefore, the neural network preformed much better in predicting the Z component and the standard deviation of the gyroscope. The overall overlap between the predicted data and actual measurement proves the capabilities of this system to predict the gyroscope data from the pilot inputs with fairly good accuracy.

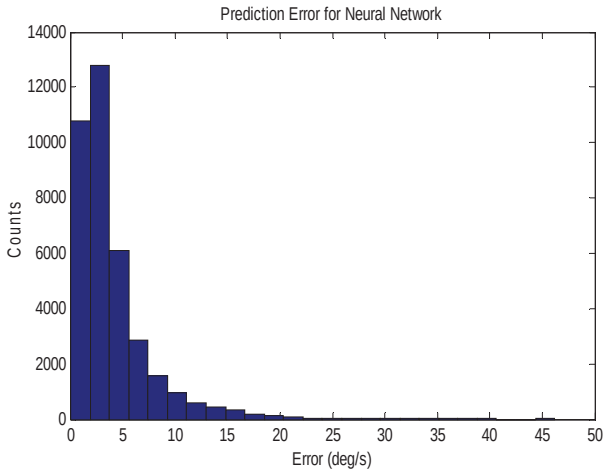

Fig. 5: Histogram for prediction error of the neural network

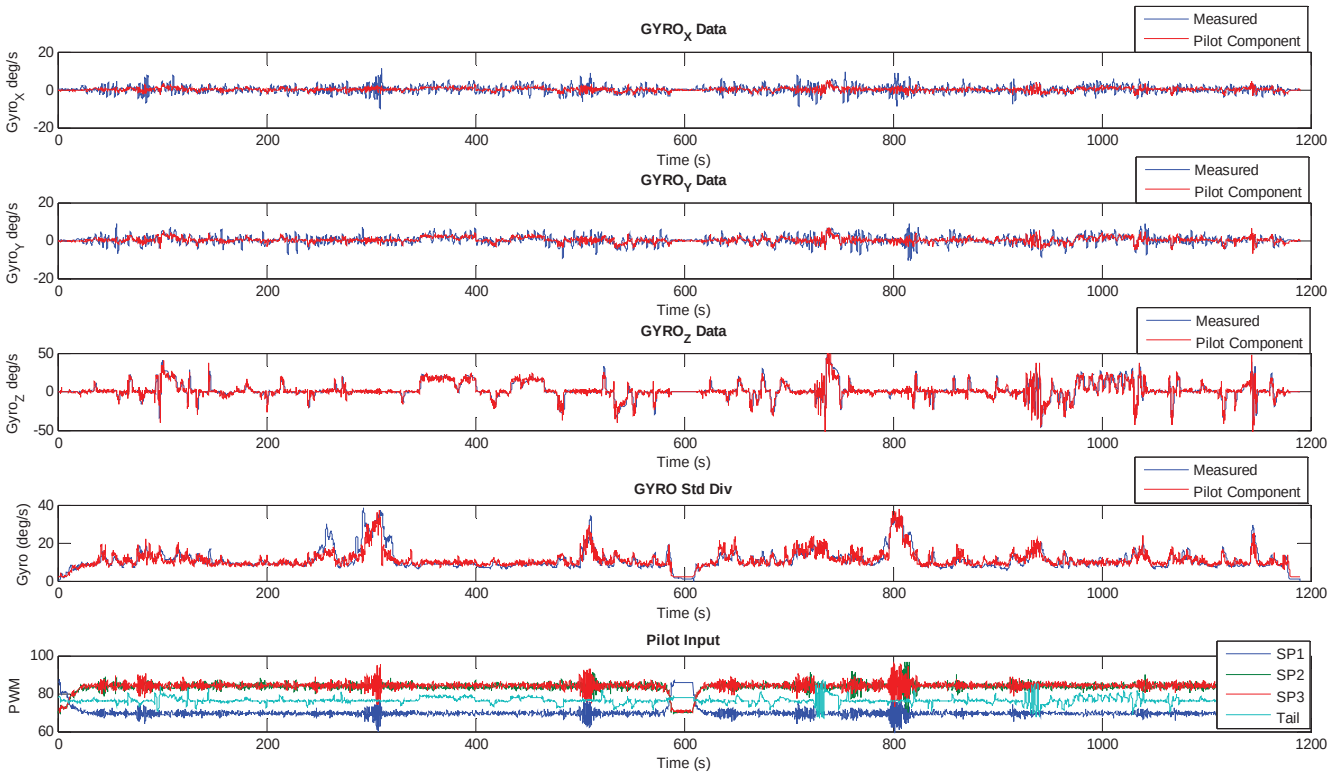

Fig. 6: Predicted gyroscope data overlaid on actual measurements

V. Air wake Measurement

High rotor speeds introduce noise in IMU readings in the form in internal oscillations. Since the frequency of such oscillations is much higher than that caused by air wake, effect of the helicopter's own vibrations in the gyroscope output can be nullified by applying a Gaussian low pass filter. If $\boldsymbol{\omega}$ is the raw gyroscope data then the filtered signal ($\boldsymbol{\omega_f}$) is obtained as follows:

$$\boldsymbol{\omega_f} = \boldsymbol{\mathcal{G}}(\sigma, L) * \boldsymbol{\omega} \tag{4}$$

where * is the mathematical convolution operation and $\boldsymbol{\mathcal{G}}(\sigma, L)$ is the Gaussian low pass filter kernel with width σ and length L. The larger the values of σ and L are,-then the lower the cut-off frequency of the filter. It is required to retain the motion of the helicopter due to air wake (whose time constant is in the order of 1 sec) and filter the high frequency noise. Therefore, L was selected to be 1 sec. Through empirical optimization, it was found that σ of 0.6 sec worked well over the wide range of data acquired.

Since the aim of this project is to determine launch and recovery envelopes for naval vessels, the direction of the air wake is less important than the magnitude of the vibrations which determine the intensity of the air wake. Therefore, it is advantageous to use radial component of the Gyroscope data rather than the three Cartesian components since it decreases the computation burden. In the proposed system, the gyroscope data was converted to a spherical coordinate system and the absolute magnitude (radial component) was used to represent the air wake pattern. If $\{\omega_x, \omega_y, \omega_z\}$ is the filtered angular velocity ($\boldsymbol{\omega_f}$) of the helicopter in Cartesian coordinate system measured from the gyroscope and $\{\omega_x', \omega_y', \omega_z'\}$ is the angular velocity determined from the Neural Network, then the radial component of the net angular velocity (ω_r) due to air wake is obtained as:

$$\omega_r = \sqrt[2]{(\omega_x - \omega_x')^2 + (\omega_y - \omega_y')^2 + (\omega_z - \omega_z')^2} \tag{5}$$

Air wake causes the helicopter to oscillate vigorously (with large amplitude), which appears as oscillations in the IMU (predominantly in the Gyroscope) data. Therefore whenever the helicopter enters into an air wake zone, an increase in gyroscope fluctuation readings is expected. This fluctuation will appear as a peak in the gyroscope absolute magnitude (radial) component as well as a peak in the local standard deviation of the gyroscope radial component. The resultant waveform is an (absolute) angular velocity of the helicopter caused by the air wake alone.

During air wake peak, the helicopter is faced with strong air wake gusts therefore one should observe sudden changes in angular/linear velocities under the effect of large accelerations. To measure the extent of changes in angular velocities, local standard deviation for the gyroscope data

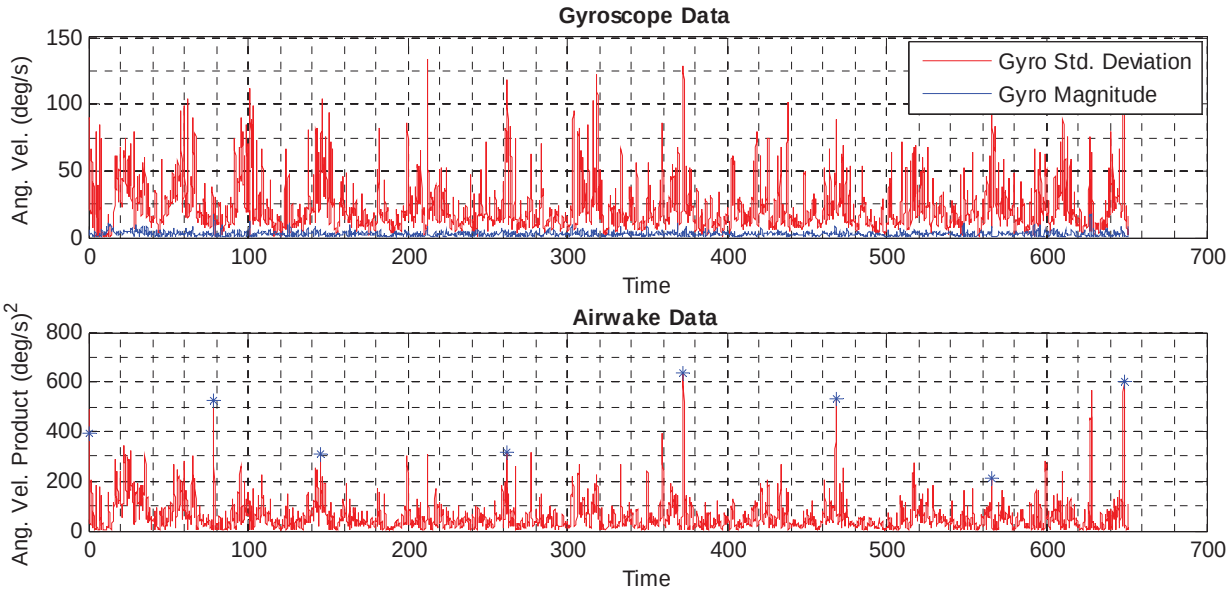

Fig. 7: Air wake data after pilot input compensation for one of the test flights.

(radial component) was calculated by applying standard deviation filter with a window size of 1 sec. The i[th] sample of local standard deviation ($\boldsymbol{\omega_s}$) of the radial component of the raw gyroscope data ($\boldsymbol{\omega}$) is calculated as follows:

$$\boldsymbol{\omega_s}(i) = \sqrt{\frac{\sum_{d=-\frac{L}{2}}^{+\frac{L}{2}}\left(\boldsymbol{\omega}(i+d) - \frac{1}{L}\sum_{x=-\frac{L}{2}}^{+\frac{L}{2}}\boldsymbol{\omega}(i+x)\right)^2}{L}}^{2} \quad (6)$$

where $i \in I\,[1, N]$ and N is total number of samples in $\boldsymbol{\omega}$.

Since a simultaneous rise is expected in the filtered gyroscope data and its standard deviation data, the two waveforms were multiplied (point-to-point multiplication) to analyze air wake conditions. Furthermore, the standard deviation ($\boldsymbol{\omega_s}$) also contains the component arising from pilot inputs; therefore, there is a need to compensate for pilot inputs in the standard deviation data while predicting air wake. For convenience, the generated waveform is referred to as the '*Air wake Data*' ($\boldsymbol{A_\omega}$):

$$\boldsymbol{A_\omega}(i) = \left(\boldsymbol{\omega_s}(i) - \boldsymbol{\omega_s}'(i)\right) \times \boldsymbol{\omega_r}(i); \quad i \in I\,[1, N] \quad (7)$$

where $\boldsymbol{\omega_s}'$ is the standard deviation of the gyro data predicted from the Neural Network. Fig. 7 shows estimation of the ship air wake data from pilot input compensated gyroscope data for one of the test flights. The upper subplot of this figure, the blue plot shows the local standard deviation of the gyro data after compensation given by equation (6) and the red plot shows the magnitude of gyro data after compensation given by equation (5). Their product referred to as 'Air wake data' given by equation (7) is shown in the lower subplot with local peaks marked in blue. Fig. 7 shows the Air Wake magnitude for the whole flight as a function of time.

Since the ship air wake magnitude is also a function of the position relative to the superstructure of the vessel, the air wake data should be associated with helicopter relative position in reference to the training vessel. The relative position of instrumented helicopter was estimated by subtracting the ship's geographic coordinates from helicopter's geographic coordinates. The relative trajectory of the helicopter was then rotated by the heading angle of the boat to project the trajectory in boat's frame of reference.

VI. Results and Conclusion

In order to test the capabilities of the proposed system, a number of test flights have been conducted in Chesapeake Bay to measure the air wake produced by YP 676 boat for relative wind angles of 0° and 15° (as measured from the bow the ship in the clockwise direction). For each test flight, the *Air Wake* data was generated and overlaid on the helicopter trajectory in the form of a color plot.

Figs. 8 and 9 show air wake distribution estimated from the proposed system for relative wind from 0° and 15° respectively. In these distribution plots, the color on the helicopter trajectory represents the air wake magnitude in the form of vibrations sustained by the helicopter. In Fig. 8, the high aiwake zone is concentrated along the center line. This is in accordance with the wind conditions and related numerical simulations [13,14]. Similarly, in Fig 9, the high air wake zone is tilted to the right, which again corresponds to numerical simulations [13,14].

Currently, the proposed system is effective for determining air wake distribution pattern which is basically a distribution of magnitude. This system can be extended to

estimate air wake direction through the use of accelerometer data and could also be potentially used for navigating an autonomous UAV. The proposed system has the potential to evolve into a wireless air flow sensor without actually measuring airflow. The authors plan to further extend this work to transmit the data wirelessly in realtime. Prediction results can be further improved by trying other existing machine learning algorithms.

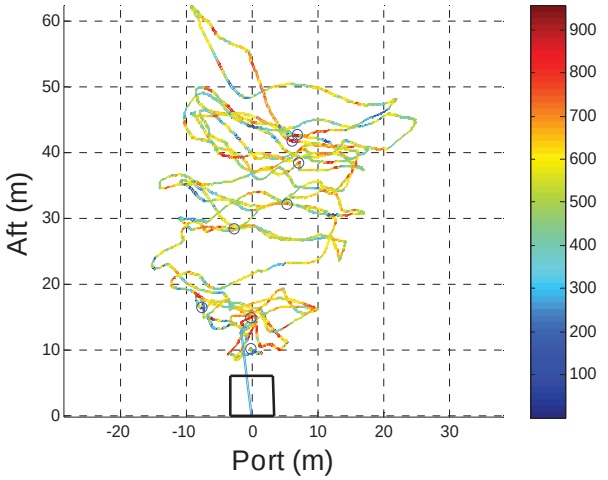

Fig. 8: Ship air wake distribution for one of the test flights with wind direction of 0°.

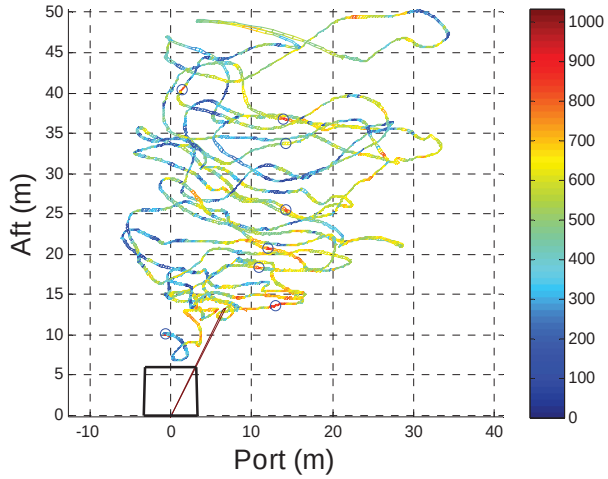

Fig. 9: Ship air wake distribution for one of the test flights with wind direction of 15°.

ACKNOWLEDGMENT

This research is supported by the Office of Naval Research (Principal Investigator M. Snyder). The authors wish to thank Sina Aghli for his help with the design and integration of the Pilot Input Receiver Module, and Wael Saab, Jeffery Phillips and YP 676 crew for their help with data collection.

REFERENCES

[1] "Helicopter operating procedures for air-capable ships NATOPS manual," NAVAIR 00-08T-122, 2003.

[2] Guillot, M.J. and Walker, M.A., "Unsteady analysis of the air wake over the LPD-16," AIAA 2000-4125: 18th Applied Aerodynamics Conference, Denver, Colorado, 2000.

[3] Lee, D., Horn, J.F., Sezer-Uzol, N., and Long, L.N, "Simulation of pilot control activity during helicopter shipboard operations," AIAA 2003-5306: Atmospheric Flight Mechanics Conference and Exhibit, Austin, Texas, 2003.

[4] Lee, D., Sezer-Uzol, N., Horn, J.F., and Long, L.N., "Simulation of helicopter ship-board launch and recovery with time-accurate air wakes," Journal of Aircraft, Vol. 42, No. 2, 2005, pp. 448-461.

[5] Polsky, S., Imber, R., Czerwiec, R., & Ghee, T., "A Computational and Experimental Determination of the Air Flow around the Landing Deck of a US Navy Destroyer (DDG): Part II," AIAA-2007-4484: 37th AIAA Fluid Dynamics Conference & Exhibit, Miami, FL, 2007.

[6] Roper, D. M., Owen, I., Padfield, G.D. and Hodje, S.J., "Integrating CFD and pilot simulations to quantify ship-helicopter operating limits," Aeronautical Journal, Vol. 110, No. 1109, 2006, pp. 419-428.

[7] Snyder, M.R., et al., "Determination of Shipborne Helicopter Launch and Recovery Limitations Using Computational Fluid Dynamics," American Helicopter Society 66th Annual Forum, Phoenix, AZ, 2010.

[8] Snyder, M.R., et al., "Comparison of Experimental and Computational Ship Air Wakes for YP Class Patrol Craft," American Society of Naval Engineers Launch and Recovery Symposium, Arlington, VA, December 2010.

[9] Miklosovic, D.S., Kang, H.S. and Snyder, M.R., "Ship Air Wake Wind Tunnel Test Results," AIAA 2011-3155: 29th AIAA Applied Aerodynamics Conference, Honolulu, Hawaii, June 2011.

[10] Snyder, M.R, Kang, H.S. and Burks, J.S, "Comparison of Experimental and Computational Ship Air Wakes for a Naval Research Vessel," AIAA 2012-2897: 30th Applied Aerodynamics Conference, New Orleans, Louisiana, June 2012.

[11] Snyder, M.R, Kumar A., Ben-Tzvi P. and Kang, H.S., "Validation of Computational Ship Air Wakes for a Naval Research Vessel," 51st AIAA Aerospace Sciences Meeting, AIAA Paper 2013-0959, Grapevine, Texas, January 7-10, 2013. DOI: 10.2514/6.2013-959.

[12] Brownell, C.J., Luznik, L., Snyder, M.R., Kang, H.S., and Wilkinson, C.H., "In situ air velocity measurements in the near wake of a ship superstructure," Journal of Aircraft, Vol. 49, No. 5, Sep.–Oct. 2012.

[13] Snyder M.R., Kang H.S., Brownell C.J., Burks J.S., "Validation of Ship Air Wake Simulations and Investigation of Ship Air Wake Impact on Rotary Wing Aircraft", Naval Engineers Journal, Vol 125, No. 1, March 2013.

[14] Metzger, J.D., Snyder, M.R., Burks, J.S. and Kang, H.S., "Measurement of Ship Air Wake Impact on a Remotely Piloted Aerial Vehicle," American Helicopter Society 68th Annual Forum, Fort Worth, Texas, May 2012.

[15] Rojas, R., "Neural Networks - A Systematic Introduction", Springer-Verlag, Berlin, New-York, 1996, pp 151-184.

[16] Haykin, S., "Neural Networks: A Comprehensive Foundation", Prentice-Hall, Englewood Cliffs, NJ, 1999.

[17] Simpson, P.K., "Artificial Neural Systems" Pergmon Press Elmsford, New York, 1989.

[18] Karnin, E., "A simple procedure for pruning backpropagation trained neural networks", IEEE Transactions on Neural Networks, 1(2), 1990, pp. 239-242.

[19] Widrow, B., and S.D. Sterns, "Adaptive Signal Processing," New York, Prentice-Hall, 1985.

[20] Kohavi, R., "A study of cross-validation and bootstrap for accuracy estimation and model selection". Proceedings of the 14th International Joint Conference on Artificial Intelligence, 1995, 2(12): pp. 1137–1143.